HEAT TRANSFER ENHANCEMENT THROUGH THE USE OF TRANSVERSE VORTEX GENERATORS

Slawomir Blonski[a], Tomasz Kowalewski[a], Dariusz Mikielewicz[b], Adam Stasiek[b], Jan Stasiek[b]

[a] *IPPT PAN, Polish Academy of Sciences, Świętokrzyska 21, 00-049 Warszawa, Poland*
[b] *Gdansk University of Technology, Department of Heat Technology,80-952 Gdansk, Poland*

ABSTRACT

Vortices and generation contain three passive elements to influence heat transfer: swirl, flow destabilization and developing viscous layers. They increase heat transfer by several hundred percent. Prior to the use of vortices to influence heat transfer it must be known how different vortices are generated and controlled and how they interact with the original or base flow and temperature field. To select the most appropriate vortex generators (VG) for a given task it is necessary to know the heat transfer and flow losses associated with the generation of a specific vortex system. The aim of the paper is to asses the state art and to induce others to join in the exploration of heat transfer control by vortices. Flow visualization and heat transfer experiments were conducted using an open low-speed wind tunnel equipped with liquid crystals thermography (LCT) and particle image velocimetry (PIV). In this work we consider five types of transverse vortex generators (TVGs) which where brought to required temperatures by hot film method. Heat transfer measurement were carried out by TLC. Pressure losses were also measured.

INTRODUCTION

Three passive mechanisms exist to increase convective heat transfer: (1) swirl, (2) flow destabilization, and (3) developing viscous layers.

Vortices and their generators incorporate all three enhancement mechanisms. Vortices swirl fluid around their axis of rotation, they induce velocity profiles which are less stable, and their generation implies flow separation and developing viscous layers [2,3]. Even though everybody knows what is meant by a vortex, namely swirling flow, an agreed upon mathematical definition of a vortex, very helpful for vortex identification, does not exist, even though vorticity $\nabla \times \varpi$, and also vortex line and vortex tube are well defined mathematically. That vortices do not only swirl but also destabilize the flow is well known for transverse vortices (TV), the Karman vortex street behind a cylinder in cross flow is probably the best known example. The destabilization effects of longitudinal vortices (LV) still under investigation. One of the reasons is that single LVs are more difficult to generate than TVs. Self-sustained oscillations associated with vortices have been exploited very little in general and specially for heat transfer purposes. The third mechanism viscous layer interruption and initiation of new developing viscous layers is implied by vortex generation. Vortices are generated by fluid friction and separation and the vortex generator (VG) surfaces generate new developing viscous layers. In addition vortices have two properties which make them even more attractive, for heat transfer manipulations. They have the tendency to last long and to have small cores which allows to influence heat transfer over long and narrow regions. Both properties follow from Helmholtz vortex theorem (1858) and its extension to viscous flow. In viscous flow vortices can diffuse but cannot start or end in the flow field and therefore have to be generated at solid boundaries by separation.

To use vortices to influence heat transfer it must be known how different vortices are generated and controlled and how they interact with the original or base flow and temperature field.

Special attention will be given to the influence of geometrical VG variations on self-sustained oscillations, flow visualization, heat transfer and pressure drop penalty.

Liquid crystals were used to determine the distribution of the surface temperature, and then evaluation of the heat transfer coefficient or the Nusselt number. The flow pattern produced by transverse vortex generators was visualized using a planar beam of double-impulse laser tailored by a cylindrical lens and oil particles. Sequential images of the particles in a cross sectional plane taken with CCD video camera from the downstream side the flow ware stored on a personal computer to obtain distributions of velocity vectors by means of the PIV method.

LIQUID CRYSTAL THERMOGRAPHY

Thermochromic liquid crystals (TLC) and true-colour digital image processing have been successfully used in nonintrusive technical, industrial and biomedical studies and applications. Thin coatings of TLC's at surfaces are utilized to obtain detailed temperature distributions and heat transfer rates for steady or transient processes.

Liquid Crystals Themography (so called LCT) have been extensively applied to the qualitative visualization of entire steady state, or transient temperature fields on solid surfaces. Since quantifying colour is a difficult and somewhat ambiguous task, application of thermochromic liquid crystals initially was largely qualitative. Application of the colour films or interference filters was tedious and inaccurate. The first application of true-colour digital image processing gave impact to qualitative and fast temperature measurements. Rapid development of image processing techniques has made it now possible to set-up inexpensive systems capable of real-time transient full field temperature measurements using TLCs.

Before the execution of a thermal or flow visualization experiment, we should recognise the characteristics of the

overall combination of the TLC, the light source, the optical and camera system, and make a rational plan for the total measurement system. The relationship between the temperature of the crystal and the measured Hue of the reflected light defines the calibration curve for the specified liquid crystal [7]. The distribution of the colour component pattern on the liquid crystal layer was measured by RGB colour camera and a series of images at different temperatures defines the calibration. Two main methods of surface temperature measurements are performed involving steady state and transient techniques. A brief history of these is given by Baughn et al [1] and Stasiek [7].

Steady State Analyses - Constant Flux Method

The steady state techniques employ a heated model and the TLC is used to monitor the surface temperature T_w, it gives the local heat transfer coefficient, h,

$$q = I^2 r \quad \text{and} \quad h = \frac{q}{T_w - T_a} \tag{1}$$

where T_a is a convenient driving gas temperature, I is the current and r is the electrical resistance of the heater.

Steady State Analyses - Uniform Temperature Method

The TLC-coated test specimen forms one side of a constant temperature water bath and is exposed to a cool/hot air flow. In this case, the heat transfer coefficient, h

$$h = \frac{k}{x}\frac{\left(T_w - T_b\right)}{\left(T_a - T_w\right)} \tag{2}$$

where, T_b is a water-side temperature of the wall, x the wall thickness and k the wall thermal conductivity.

Transient Method

This technique requires measurement of the elapsed time to increase the surface temperature of the TLCcoated test specimen from a known initial temperature predetermined value. Leiner et al, see [7] developed the formula for evaluation of heat transfer coefficient h:

$$h = -\frac{\delta \rho c}{t} \ln\left[\frac{T_a - T}{T_a - T_i}\right] \tag{3}$$

where, δ is a plate wall thickness and the transient local surface temperature T is detected after a time interval t, ρ and c are the model density and specific heat, T_i and T_a are the initial wall and air temperatures and t is time from initiation of the flow.

Experimental Apparatus

The experimental study was carried out using an open low-speed wind tunnel consisting of entrance section with fan and heaters, large settling chambers with diffusing screen and honeycomb, and then working sections Fig. 1. Air is drawn through the tunnel using a fan able to give Reynolds numbers of between 500 and 40 000 . The working air temperature in the rig ranges between 15°C to 65°C produced by the heater or cooler positioned just downstream of the inlet. The major construction material of the wind tunnel is perspex. Local and mean velocity are measured using conventional Pitot tubes and DISA hot-wire velocity probe.

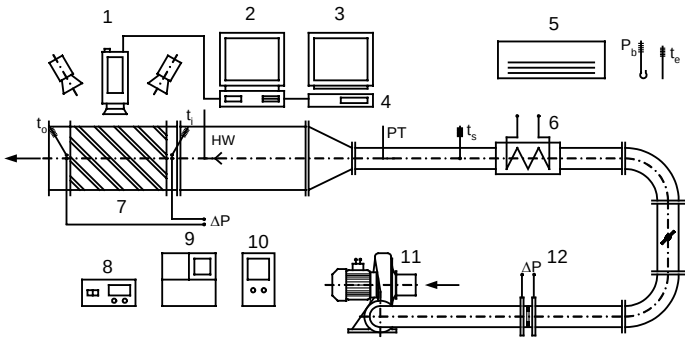

Figure 1. Open low speed wind-tunnel, 1 – RGB camera (TK-1070), 2 – PC, 3 – monitor (RGB-VMR 200), 4 – S-VHS recorder, 5 – air conditioning system, 6 – heater, 7 – LC mapping section, 8 – digital micro manometer FCO 12, 9 – DISA hot wire system, 10 – variac, 11 – fan, 12 – orifice.

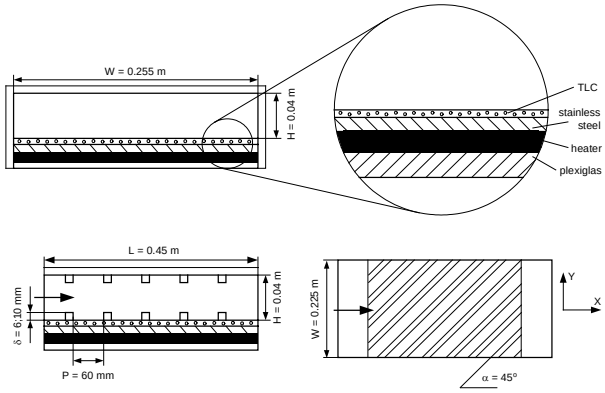

Figure 2. Schematic diagram of the rib turbulator test surfaces

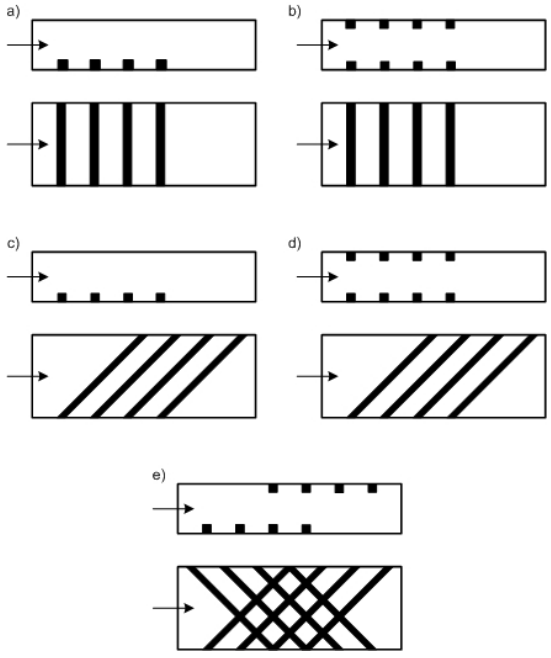

Figure 3. Five types of transverse vortex generators (cross-corrugated and rectangular ribs)

The alternative effects of constant wall temperature and constant heat flux boundary conditions are obtained using electric heater. Photographs are taken using a RGB video-camera and a true-colour image processing technique.
The liquid crystals used here manufactured in sheet form by Merck Ltd [9] had an event temperature range of 30,0 – 35,0 ^{o}C. In this particular experiment uncertainty was estimated as about ± 0,05 ^{o}C by considering only the section of the surface used in the experiment, span-wise non-uniformities in Hue value are minimized.

PARTICLE IMAGE VELOCIMETRY (PIV)

Particle Image Velocimetry technique is a well-established experimental method in fluid mechanics, that allows quantitative measurement of two-dimensional flow structure. It enables the measurement of the instantaneous in-plane velocity vector field within a planar section of the flow field and allows to calculate spatial gradients, dissipation of turbulent energy, spatial correlations, and the like [6]. In PIV technique selected cross-section of the investigated seeded flow is illuminated by laser light formed in thin "light sheet" (Fig.4). Images of the flow are recorded by CCD camera and correlated to calculate instantaneous velocity fields.

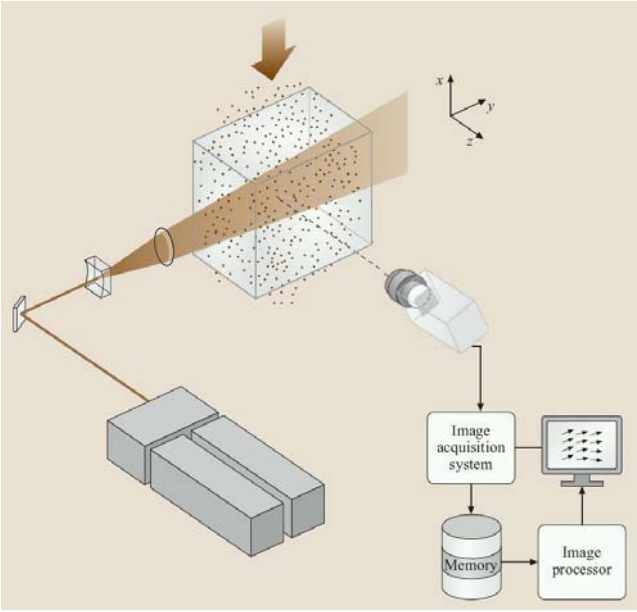

Figure 4. Schematic of a typical PIV measurement system

The main part of the experimental set-up (Fig. 4) consists of a transparent model of ribbed channel, laser light source (30 mJ double pulse Nd:YAG laser *SoloPIV, New Wave Research, Inc.*) and high resolution 12bit digital CCD camera (1280 × 1024 pixels, *PCO SensiCam*). This system permits acquisition of two images at the minimum time interval of 200ns, exposition time of 5ns, and about 3.75Hz repetition rate. The PIV recording system installed on 3GHz Pentium 4 computer with 3GB RAM capable for acquisition over 200 pairs of images during a single experimental run.
The PIV measurements were performed for pure air seeded with small droplets (few micrometers in diameter) of synthetic oil DEHS (Di-Ethyl-Heksyl-Sebacat). The oil drops volumetric concentration was very low (< 0.001), hence they did not affect the flow structure.

EXPERIMENTAL RESULTS AND DISCUSSIONS

Experimental results - LCT

In many cases, as mentioned above, remarkable enhancements of local and spatially averaged survace heat transfer rates are possible with rib turbulators, in spite of the lower local Nusselt number at certain locations along the ribbed surfaces. Fig. 2 shows the geometric details of the rib turbulator test surface. Prior to this ribbed turbulator test section is a 255x40 mm inlet duct that is 550 mm in length. This is equivalent to 7,96 hydraulic diameter (where the hydraulic diameter is 69,11 mm). The test surface that is analyzed contains a collection of rib turbulators that are parapendicular and angled with respect to the flow stream (Fig 3). To determine the surface heat flux (used to callculate heat transfer coefficients and Nusselt numbers), the convective power levels provided by the thermofoil heaters are divided by flat test surface area. Spetially resolved temperature distributions along the bottom rib turbulator test surface are determined using liquid crystals thermography (LCT) and true-colour image processing system commercially available from Data Translation Inc. [8].
In the discussion that follows, the Nusselt number

$$Nu = h \cdot \frac{D_h}{k} \tag{4}$$

Where h is the heat transfer coefficient, D_h is the channel hydraulic diameter and k is the molecular thermal conductivity of air.
The heat transfer coefficient is then bases on the flat projected area and is determined using

$$h = \frac{q_n}{(T_w - T_\alpha)} \tag{5}$$

where q_n is the local (net) surface heat flux, local surface temperature T_w (found from LCT) and T_α is the time – averaged, local mixed mean air temperature.

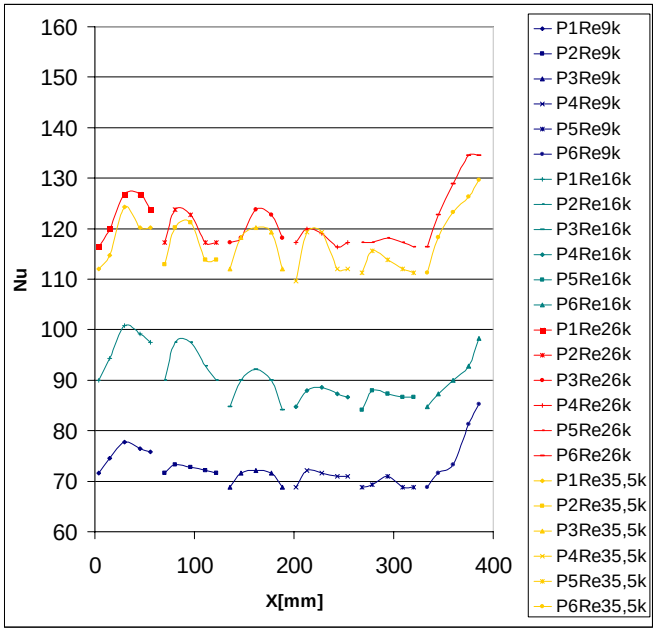

Figure 5. Nusselt number distribution in consecutive test section with a ribbed walls (Re=9000, 16000, 26000 and 35500) and perpendicular flow to ribs.

The surface Nusselt number distribution along the rib turbulator test surface are presented in Fig 5. for four Reynolds number and geometry 3a. It is evidence that transverse vortex generators (TVG_s) enhance heat transfer by several hundred percent but only for certain Reylonds number. Comparison between the maps of velocity vectors and local Nusselt numbers contours reveals that high velocity do not enhance heat transfer in some cases, probably moving fluid (with high velocity) do not penetrates into the boundary layer and flow above ribs. Optimum flow condition should be established for high efficient enhancement of heat transfer augmentation in particular environment e.g. flow and heat exchanger configuration.

Experimental results - PIV

As results, 18 sets of velocity fields were obtained from the PIV measurements: for different ribs geometries and different Reynolds numbers (Re = 9000, 16000 and 26000). The area interrogated by the PIV method was in all cases located in the mid-vertical-plane between side walls.

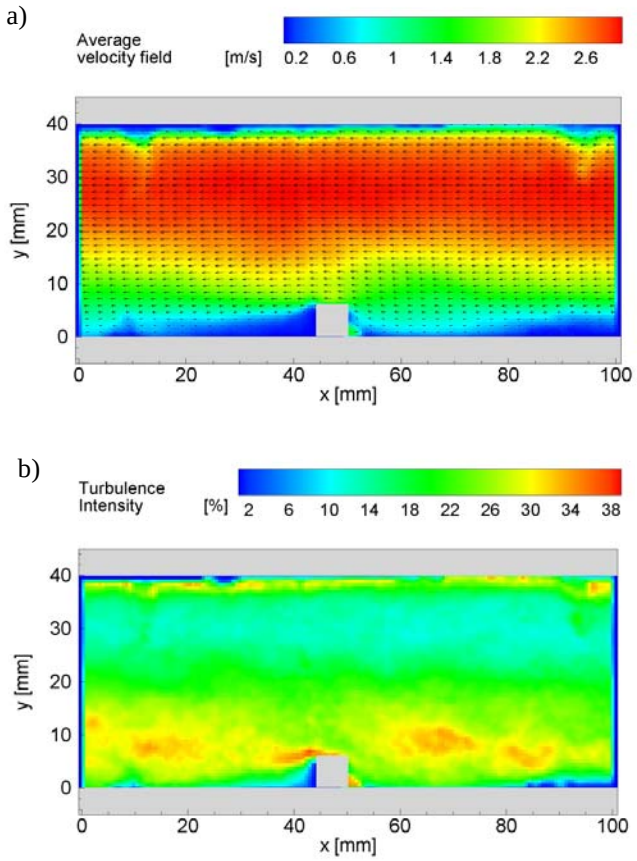

Figure 6. Averaged velocity field (a) and turbulence intensity (b) for geometry with ribbed bottom wall and Reynolds number Re = 9000.

Figure 6a shows average velocity field (averaged over 100 instantaneous velocity fields) for geometry with ribbed bottom wall, only and Reynolds number Re = 9000. Maximum velocity for this case is about 3m/s and is located in the top part of the channel. Presented averaged velocity filed seems to be quite smooth but computed from 100 instantaneous velocity fields turbulence intensity (Fig. 6b), defined as:

$$I = \frac{\left(\frac{1}{n}\sum_{i=1}^{n}\left(u_i - \overline{u}\right)^2\right)^{\frac{1}{2}}}{\overline{u}} \cdot 100\%, \qquad (6)$$

where u_i and $\overline{u}$ are instantaneous and average velocity fields, respectively and n is a number of measurements, shows that flow is turbulent with maximum turbulence intensity about 38% in the vicinity of the rib and relatively small turbulence intensity in top part of the channel (about 10%).

Figures 7a and 7b show the same fields but for Reynolds number Re = 26000. Maximum velocity is here about 8m/s and is located also in the top part of the channel. Turbulence intensity field, presented in figure 3b, shows that this intensity achieves maximum value (about 40%) in the vicinity of the rib and decreases to 14% in top part of channel.

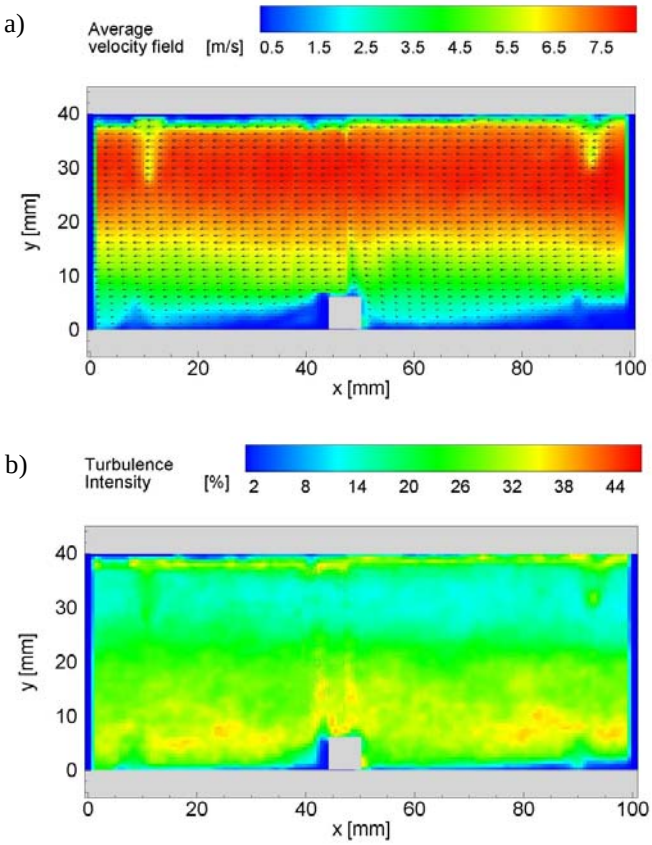

Figure 7. Averaged velocity field (a) and turbulence intensity field (b) for geometry with ribbed bottom wall and Reynolds number Re = 26000

CONCLUSIONS

A new experimental technique, in this case true-colour image processing of liquid crystal pattern and particle image velocimetry allows new approaches to old problems and the same time opens up new areas of research. Image processed data makes available quantitative, full-field information about the distribution of temperature, flow visualization and heat trnansfer coefficient, which will undoubtedly encourage the study of situation which have been, until now, too complex to consider. Future work will involve applying the present methods to more complex geometry and unsteady flow.

ACKNOWLEDGEMENT

The work reported in this paper includes scientific cooperation between University of Genoa, Italy, Center Mechanics, IPPT PAN, Warszawa, Poland and Gdansk University of Technology, Gdansk, Poland. The financial assistance of Ministry of Science and Higher Education, Poland, Grant No. 3T10B07329 is kindle acknowledged.

REFERENCES

[1] J.W. Baughn and X. Yan. Liquid Crystal Methods in Experimental Heat Transfer. Proc. 32nd Heat Transfer and Fluid. California: Mechanics Institute Sacramento, pp 15-40, 1991

[2] M. Fiebig. Vortices: Tools to Influence Heat Transfer – Recent Developments, Proc. 2nd European Thermal Sciences and 14th UIT National Heat Transfer Conference. pp 41-56, 1996

[3] M. Fiebig. Vortex Generators for Compact Heat Exchangers. J. of Enhanced Transfer Vol.2, pp 43-61, 1995

[4] T. A. Kowalewski, P. Ligrani, A. Dreizler, C. Schultz and U. Fey in C. Tropea, J. Foss and A. Yarin (ed.), Handbook of Experimental Fluid Mechanic, Chap. 7, Springer-Verlag, Berlin, Heidelberg 2007

[5] R. J. Moffat. Experimental Heat Transfer Proc. The Ninth International Heat Transfer Conference, Jerusalem, Israel pp 187-205, 1990

[6] M. Raffel, C. Willert, J. Kompenhans. Particle Image Velocimetry, A Practical Guide, Springer-Verlag, Berlin, 1998

[7] J. Stasiek, A. Stasiek, M. Jewartowski and M. W. Collins. Liquid Crystal Thermography and True-Colour Digital Image Processing. Optics & Laser Technology, Vol. 38, pp 243-256, 2006

[8] DATA TRANSLATION Ltd.: Image Processing Handbook, 1991

[9] MERCK Ltd. Thermochromic Liquid Crystals. Broom Road, Poole, U.K.

[10] MINCO Products, Inc., Minnesota, USA